Dicarboxylic acid-epoxy vitrimers: influence of the off-stoichiometric acid content on cure reactions and thermo-mechanical properties

Quentin-Arthur Poutrel, Jonny J Blaker, Constantinos Soutis, François Tournilhac, Matthieu Gresil

Dicarboxylic acid-epoxy vitrimers: Influence of off-stoichiometric acid content on cure reactions and thermo-mechanical properties

Quentin-Arthur Poutrel,[a,b] Jonny J Blaker,[a] Constantinos Soutis,[b] François Tournilhac*[c] and Matthieu Gresil*[d]

[a.] *Bio-Active Materials Group, Department of Materials, The University of Manchester, Manchester, UK.*
[b.] *Aerospace Research Institute, The University of Manchester, Manchester, UK.*
[c.] *Molecular, Macromolecular Chemistry, and Materials, CNRS, ESPCI, PSL Research University Paris, France.*
[d.] *i-Composites Lab, Department of Materials Science and Engineering, Monash University, Clayton, Australia.*
†

Manuscript published in Polymer Chemistry 2020, 11 5327-5338, DOI: 10.1039/d0py00342e
Electronic Supplementary Information (ESI) available: Manufacture of vitrimer networks, IR analysis method, dynamic mechanical analysis, mechanical results, stress relaxation results, creep results for all samples. See http://www.rsc.org/suppdata/d0/py/d0py00342e/d0py00342e1.pdf

The present study explores a broad range of stoichiometry, with [epoxy]/[acyl] ratio in excess to unity for a commercial diepoxide/sebacic acid vitrimer formulations with 1,5,7-triazabicyclo[4.4.0]dec-5-ene (TBD) used as catalyst. In particular, it investigates to what extent side reactions promoted by off-stoichiometry mixtures can achieve desirable thermomechanical properties (i.e. glass transition T_α, Young's modulus, strain at break, and strength) for an optimised vitrimer that behaves like a stiff material at room temperature, keeping its capacity to flow at high temperature while remaining insoluble. Possible role of TBD as anionic initiator is tested on the homopolymerisation of the epoxy and compared to a known anionic initiator, 2-phenylimidazole (2-PI). Attenuated total reflection infrared (ATR-IR) spectroscopy reveals different reaction speeds, but identical scenario for either 2-PI or TBD. The acid + epoxy addition occurs first, then epoxy homopolymerisation takes place after di-carboxylic acid consumption; ester typically forms in less than 20 min at 125°C with TBD, while ether takes several hours. For all [epoxy]/[acyl] ratios ranging from 1:1 to 1:0.3, it is found that the integrity of the network remains while submitted to 1,2,4 trichlorobenzene (TCB) solvent. From 1:1 to 1:0.75 epoxy to acyl ratio, the material keeps full ability to flow and relax stresses under thermal stimulation, showing a 10 fold increase of viscosity and unchanged activation energy of about 100 $kJ.mol^{-1}$. Beyond stoichiometry 1:0.6, a gradual transition from vitrimer to non exchangeable crosslinked materials is observed as these networks show only partial stress relaxation due to interpenetration with polyether network.

Background

Polymer networks with reversible covalent links have been investigated as systems that are capable of topology rearrangement in response to excitation[1, 2] (thermal or photochemical activation), as reviewed in the last 6 years.[3, 4] Systems where reversibility involves chemical reactions going through a dissociative mechanism like the Diels-Alder reaction,[5] were first studied due to the wide range of chemical reactions available.[6, 7] In these systems, the dissociative mechanism means that whenever topology rearrangement is desired, former links have to be broken before new links can be established, leading to a temporary drop of viscosity and loss of structural integrity once bond reversibility is activated. In contrast, a different family of reversible covalent networks can be envisioned where the creation of new bonds takes place before former ones are broken, thus maintaining the integrity of the network throughout the exchange process. In 2005, Bowman and coll.[8] described photo-induced plasticity in crosslinked polymers based on reversible chain-transfer reactions involving an associative mechanism, and, in 2011, Leibler and coll.[9] introduced the concept of vitrimers – a class of polymer networks with dynamic links and/or crosslinks that became the example of associative exchange reactions upon thermal excitation. Vitrimers are insoluble thermoset-like polymers. Under thermal stimulation, bond exchanges are rapid, especially in the presence of a well-chosen catalyst. Thereby, the material can flow through reorganisation of network topology; thus they have been proven to be heat-processable, recyclable and weldable, akin to thermoplastics.[10-12]

The present concept (i.e. covalent bond exchange) is not linked to any particular chemistry. In vitrimer prototypes, the possibility of building dynamic poly-hydroxyl ester networks by thermoset chemistry has been demonstrated.[9] Since then, numerous examples of vitrimers based on various skeletons and involving a large choice of exchange reactions, with and without catalysts, have been described.[13-22] Nonetheless, the epoxy chemistry used in the initial vitrimers remains appealing since it is based on a choice of industrially relevant monomers. Epoxy resins are heavily used in transport-, health-, electronic-, and energy-related technologies. Currently, a wide range of epoxy monomers and hardeners are commercially available or at least well described in the literature,[23, 24] and virtually any combination of each is possible. Epoxy curing is an ensemble of ring-opening reactions with the ability to operate without solvent, without by-products – not even a molecule of water – and with low shrinkage.[25, 26] Esterification and transesterification are among the most common reactions of organic chemistry, used on a large scale to produce[27] (and recycle) polyesters[28] and, more recently, in bio-diesel production[29], for which a vast literature of reaction conditions and catalysts are available.[30-34]

Epoxy based vitrimers are relatively new material systems that can be employed as matrix in fibre reinforced composite materials.[35, 36] However, so far, the glass transition – an intrinsic property of thermosets noted T_g (measured by DSC) or T_α (measured by DMA) – remains difficult to predict by any other method than trial and error. Often efforts to increase T_g (or T_α)

above a certain value (depending of network compounds and curing conditions), cause issues with the entire formulation in terms of compatibility, processing, degassing, and curing cycles.[37]

Epoxy-carboxylic acid vitrimer formulations reported in the literature to date[9, 38-40] have mostly used a 1:1 epoxy to acyl ratio. The addition of one -COOH group onto the epoxy ring generates one hydroxide for each ester formed, giving an equal concentration of both reactants for further exchanges by transesterification. Decreasing the epoxy to acyl ratio to 1:2 has been reported for some epoxy-anhydride formulations, in all cases a decrease in weldability was observed.[10, 35] The present work explores the effect of varying the stoichiometric ratio in the opposite direction, i.e. towards increasing the epoxy to acyl content. Altuna et al.[41, 42] have shown that decreasing the acid content could lead to the formation of ethers through anionic homopolymerisation of the remaining epoxy as suggested by Matejka et al.[43] in the early 80s. Torkelson and coll.[44] synthetised vitrimers containing a maximum of 40% fraction of permanent crosslinks to increase creep resistance. Hoppe et al.[45] analysed the reaction of DGBEA with a stoichiometric amount of monocarboxylic acid and also with a variable excess of epoxy groups with a conventional tertiary amine as catalyst. They obtained a gel when the ratio epoxy to acid groups was higher than 3, but with a drop of *Tg* from 90 to 0°C. Recently, Altuna et al. [46] synthesised poly hydroxy-ester vitrimer networks with a fraction of non-exchangeable amine links as internal catalysts in the network, they developed a statistical analysis of the network structure to estimate the partition of the tertiary amine between sol and gel fractions.

Here, the effect of non-stoichiometry on vitrimer properties is investigated. In our experiments, epoxy vitrimer samples have been manufactured, comprised of a commercial epoxy resin (mixture of diepoxide monomers) and sebacic acid (SA) as hardener, with different stoichiometries (From 1:0.3 to 1:1 epoxy/acyl ratio), and organic catalyst 1,5,7-Triazabicyclo[4.4.0]dec-5-ene (TBD).

Table 1 Reactant used in this study; eew: epoxy equivalent weight, mw: molecular weight, ROP: ring opening polymerisation

Chemical structure	Compound	Acronym	M (g/mol)
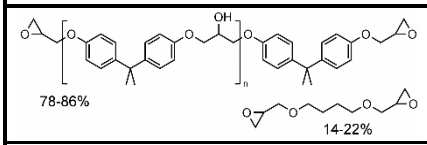	Diepoxide monomer (LY564)	DE	172-176 (eew)
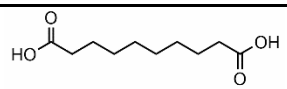	Diacyl monomer (sebacic acid)	SA	202.2 (mw)
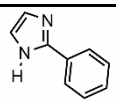	Initiator of anionic ROP (2-phenylimidazole)	2-PI	144.2 (mw)
	Transesterification catalyst (1,5,7-triazabicyclo[4.4.0]dec-5-ene)	TBD	139.2 (mw)

Materials and methods

Araldite LY 564 was chosen for its versatility as a low-viscosity resin for a variety of applications, including materials for electronics or structural composites. Sebacic acid is a classic bio-based molecule, used as monomer in polyamide chemistry and already proven in epoxy vitrimer formulations.[41, 46-48] TBD is a well-known transesterification catalyst with guanidine structure, including secondary, tertiary amine, and imine functions.[49] Its structure makes it a strong base, potentially initiating anionic ring-opening polymerisation (ROP)[50] of epoxides. For comparison, mixtures of the diepoxide with 2-phenyl-imidazole (2-PI), which is known as an effective anionic initiator were also investigated. The structures of the monomers and catalysts are shown in Table 1 and the electronic supplementary information (ESI) Scheme S1.

Sample preparation

The diepoxide monomer (DE) - Araldite LY564 - was purchased from Huntsman Ltd; sebacic acid (SA) 2-phenyl-imidazole (2-PI) and 1,5,7-triazabicyclo[4.4.0]dec-5-ene (TBD) were supplied by Tokyo Chemical Industry Ltd Belgium. Sebacic acid and TBD were added to the epoxy as received and mixed for 24 h at 50°C until a white homogeneous liquid was obtained. The final mixture was then poured into moulds, to give rectangular 60 mm × 60 mm × 5 mm, and dog-bone specimens measuring 115 mm × 33 mm × 6 mm, according to ASTM standard 638 Type IV. The samples were degassed under vacuum for 2 h at 90°C to ensure removal of possible air bubbles created during mixing. Samples were cured at 145°C for 8 h (ramp 1.7°C/min from room temperature to 145°C), and then post-cured at 160°C for 8 h. A schematic of sample fabrication is shown in Fig. S1.

A series of samples was produced with different epoxy/SA ratios (summarised in Table 2). The reaction was conducted using the 1:1 ratio of functional groups of epoxy to sebacic acid in the presence of TBD added as 5% molar equivalent (meq) of the epoxy group. The resulting material system was labelled 100H 5CAT. Samples were produced with different epoxy/SA ratios to explore

the effect of reducing the acid content in the vitrimer, as follows: 1:0.75, 1:0.6, 1:0.5, and 1:0.3 the respective materials labelled as 75H, 60H, 50H and 30H. All reactive mixtures in this series were prepared using 5% meq TBD relative to the epoxy group, except one with 10% meq TBD following the work of Leibler and coll.,[31] labelled as 5CAT and 10CAT, respectively (Table 2).

Table 2 Sample identification based on epoxy/sebacic acid ratio and catalyst amount

Samples label						
	100H5CAT	75H5CAT	60H5CAT	50H5CAT	30H5CAT	30H10CAT
DE (meq)	100	100	100	100	100	100
SA (meq)	100	75	60	50	30	30
TBD (meq)	5	5	5	5	5	10

IR monitoring of the curing process

Attenuated total reflection infrared spectroscopy (ATR-IR**)** was conducted using a SPECAC high-temperature golden gate ATR cell mounted on a Bruker Tensor 37 IR spectrometer. Curing took place at 125°C and the IR data collected during the first 60 minutes of the process, observing the change of mixture composition. Samples with 5% catalyst were studied with different epoxy/acid ratio (100H, 50H and 30H). For this study, most relevant information was found in the 900-2000 cm^{-1} wavenumber range shown in Fig S2. Due to overlap of signals, monitoring was performed through integration of absorbance over well-defined intervals. The method of analysis for ATR IR curing and integration of relevant IR signatures can be found in the ESI (Fig. S2-S5).

Swelling and soluble fraction analysis

Swelling studies were performed using samples measuring approximately 5 mm × 5 mm × 3 mm. Samples were weighed and their dimensions measured before being immersed in 1,2,4 trichlorobenzene (TCB) at 135°C (well above the T_α of the samples), after 3 days and 1 week to ensure that swelling equilibrium has been reached. TCB was chosen for its high vaporisation temperature (214°C). Swollen samples were extracted, wiped with tissue, and stabilised at room temperature for 2 days to avoid any thermal expansion effects; Swelling ratio and soluble fraction were calculated by gravimetry for all samples.

Mechanical test methods

Dynamic mechanical analysis (DMA) and creep experiments were performed using a Q800 DMA (TA Instruments, USA) operating in dual cantilever mode on rectangular samples (55 mm × 15 mm × 4 mm) with a heating regime of -30°C to 200°C at 3°C/min, and a measurement frequency of 1 Hz following standard procedures to measure the glass transition temperature (T_α).

Stress relaxation experiments were conducted using a Q800 DMA (TA Instruments, USA) operating in shear mode on rectangular samples (50 mm × 50 mm × 4 mm) with 1% strain applied and allowed to relax for 500 min at each temperature level. Temperature parameters have been adapted for each sample type according to their mechanical properties.

Creep testing was performed on rectangular samples (55 mm × 15 mm × 4 mm) cut from larger plates to observe bulk relaxation. A dual cantilever clamping system was chosen to minimise the noise due to measurement. Measurements were performed at several temperatures (from 110°C to 190°C every 10°C). Samples were heated and left to equilibrate at 110°C for 10 min prior to applying a stress of 10 kPa (100H5CAT), 1Mpa (30H10CAT) or 100 kPa (others) for 30 min to reach the regime of linear time variation .[31] They were then left to relax for 10 min and heated to the next temperature level.

Quasi-static tensile tests were performed using 3 dog-bone specimens (115 mm × 33 mm × 6 mm) for each composition, using an Instron 5969 model testing machine, equipped with a 2 kN load cell, following ASTM standard 638 Type IV. Samples were tested at 25°C using a displacement rate of 3mm/min to obtain the entire stress-strain response and elastic modulus.

Results

Analysis of vitrimer curing by ATR-IR

In effort to gain a better understanding of the network formation, infrared spectral analysis of sample curing was performed via ATR-IR. A typical IR spectrum of test sample 100H5CAT during curing is presented in Fig. 1, where the peaks of interest are highlighted. At the beginning of the experiment, already two C=O stretching bands are detected at $\bar{\nu} \approx 1705$ cm^{-1} and $\bar{\nu} \approx 1735$ cm^{-1}. The first is the conventional signal of a carboxylic acid in the molten state. The second, whose relative intensity increases with dilution (see ESI) is due to interaction with the solvent (here, the epoxy resin plays the role of the solvent).[51] Once the reaction with epoxy starts, the absorption at 1705 cm^{-1} diminishes, while absorption at 1735 cm^{-1} increases, due to the C=O stretching signal of the ester, (overlapped with the solvated COOH one). In parallel, the decay of the characteristic epoxy peak ($\bar{\nu} \approx 914$ cm^{-1}) was observed. The measurement of this signal is particularly important in samples with low acid content since it assists to understand how epoxide groups react with an off stoichiometric amount of acyl groups.

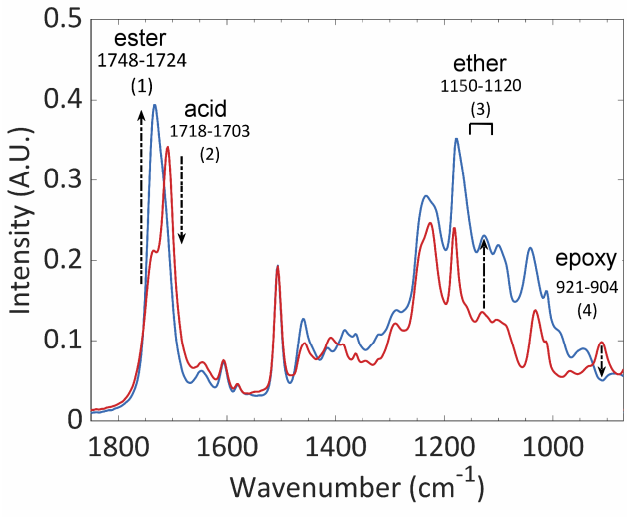

Fig. 1 ATR-FTIR spectral curve of sample 100H 5CAT at the beginning (red curve) and at the end of reaction (blue curve). The labelled peaks correspond to: (1) C=O stretching of ester related to polymer network, (2) C=O stretching of sebacic acid, (3) C-O-C signature of the ether, (4) asymmetric epoxy deformation. The numbers indicate signal integration intervals, see ESI for details of identification and integration procedure.

As for polyether formation, it is challenging to identify a single peak to characterise the homopolymerisation of the epoxide due to the complexity of the infrared absorption pattern, especially when several single C-O bonds are present. However, by analysing the whole range of C-O stretching vibration ($\bar{\nu} \approx 1000 - 1200$ cm^{-1}) it is possible to extract a C-O-C signature and follow its relative change in different reactive mixtures (see ESI).

The relative change of the defined peaks over time is shown in Fig. 2 (100H5CAT and 30H5CAT). In Fig. 2a, it can be seen that acid (blue curve, triangles) and ester (red curve, squares) signals follow complementary evolutions. The acid signal shows rapid conversion to ester during the first fifteen minutes, but the reaction continues and is still not completed after 60 min of curing at 125 °C. In Fig. 2b, the signal from the epoxy (green curve, diamonds) decreases regularly throughout the first hour of curing. The ether signal (purple curve, disks) increases slowly over the time. Thus, under the conditions of 1:1 stoichiometry, the acid + epoxy -> ester addition is predominant. Fig 2c, 2d, show the evolution of the same signals for 30H5CAT. For this off-stoichiometric formulation, the acid + epoxy -> ester addition reaction is clearly accelerated by the excess of epoxy; a horizontal asymptote is reached after 12-15 min. Interestingly, the etherification (Fig. 2d) does not start until the addition reaction is completed and ultimately it reaches a higher level than in compound 100H5CAT. In parallel, the signal from the epoxy (Fig. 2d) which participates in both reactions shows a regular decrease, slower than in 100H5CAT as expected from the law of mass action.

At 125°C, conversion is less than complete after 1 hour of curing. A long cure (8h at 145°C) was performed for all samples to achieve optimal conversion. Analysis of epoxy residuals for different stoichiometries is reported in ESI Fig S5. It appears that even for low acid content (1:0.3), almost all epoxy groups have been consumed at the end of the reaction as shown in Fig. S5. This suggests that even at highly unbalanced stoichiometry, residual unreacted monomers concentration remains constantly low.

In all formulations, a postcure is then necessary (e.g. 3000 s at 150°C)[52] to allow equilibration of the network by transesterification reactions as reported by Altuna et al[41, 42] but this cannot be detected by IR spectroscopy as it does not change the nature of chemical bonds.

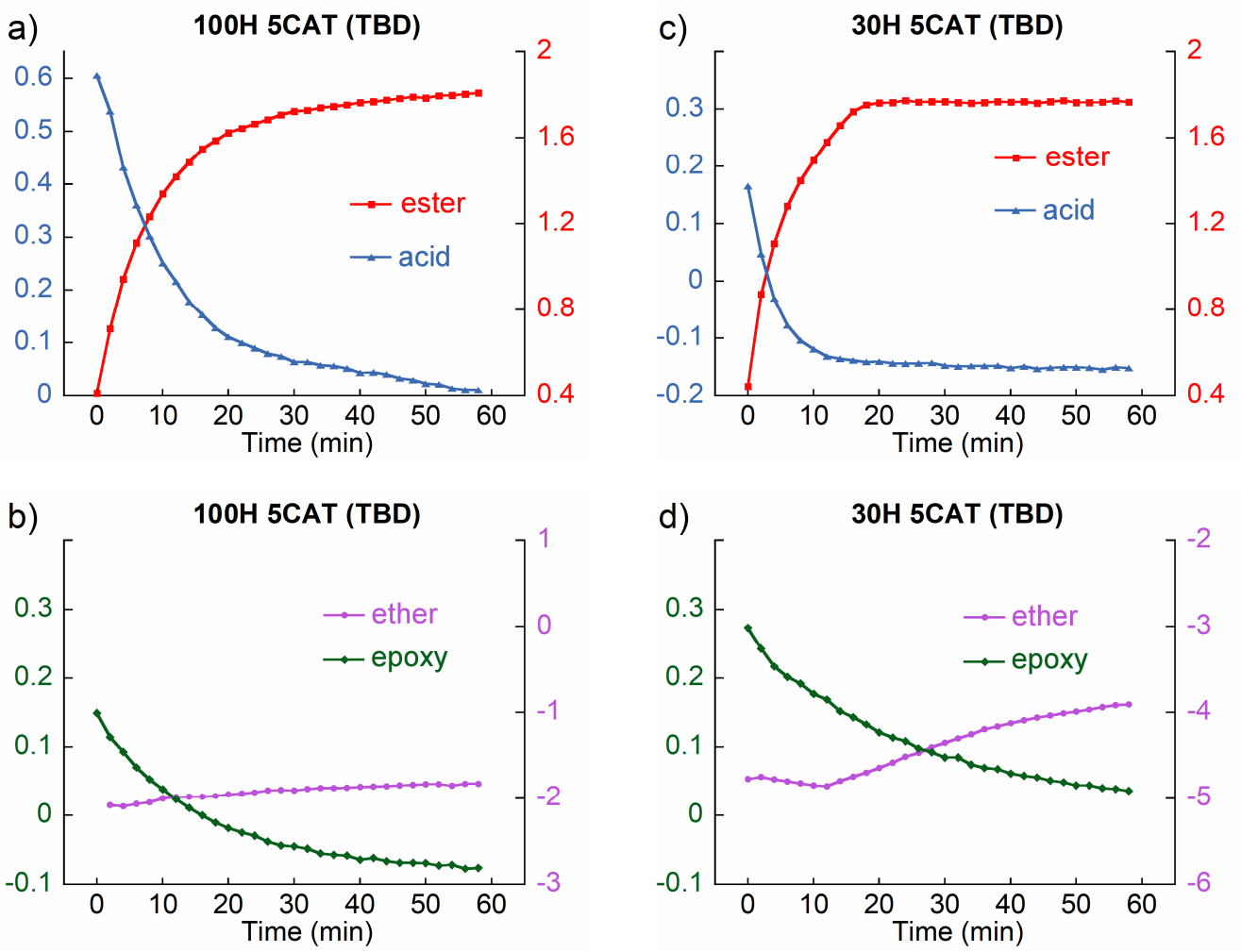

Fig. 2 Evolution of species for different ratios of polymer network a,b) 100H 5CAT, c,d) 30H 5CAT. Measurements were performed for 60 min at 125°C; Y-scales for each of the signals correspond to the values of ATR peak integrals (without normalisation, see Fig 1 and ESI for details) .

The question then arises whether such unbalanced systems can form a network. In our system, four main polymerisation reactions can be considered:

1. Poly-addition acid + epoxy forming a linear polyhydroxylester (accelerated by the TBD as shown in Fig. 2a)
2. Ficher esterification between free hydroxyl group and acid forming ester with release of water (not detected in our experiments)
3. Transesterification reaction between ester bonds and hydroxyl radicals (catalysed by the TBD, not detectable by FTIR but demonstrated in literature from small molecule studies)[52, 53]
4. Anionic ring opening polymerisation (ROP) between epoxy groups forming ether bonds[41, 42] (here initiated by the TBD)

Regarding reaction 1 (illustrated in scheme 1), the two monomers are bifunctional (diacid and diepoxy). This reaction essentially leads to linear products, whose molar mass is determined by conversion and feed ratio values; virtually infinite molar mass being achievable only at exact stoichiometry. If reaction 1 (polyaddition) were the only one to occur, the gel point would not be reachable, even more, in off-stoichiometry conditions. In this case, the material properties would be expected to range from low viscous oil to entangled thermoplastic polymer ones.

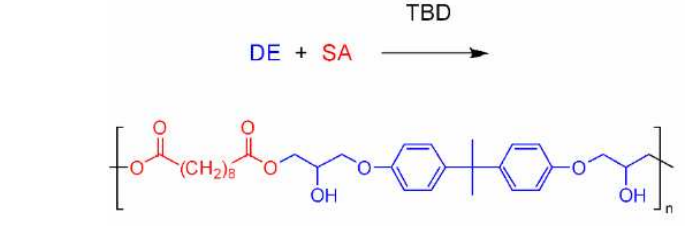

Scheme 1 Formation of exchangeable hydroxylester links by poly-addition of DE and SA.

Reaction 2, 3, and 4 are all expected to produce branching, potentially leading to a crosslinked polymer. Reaction 2 would require opposite off-stoichiometry conditions (excess of SA) and an acidic environment to take place. It is unlikely to occur in reactive mixtures catalysed with TBD (inducing a basic environment).
Branching by reaction 3 (transesterification), as illustrated in Scheme 2 is likely to occur in the presence of TBD but occurrence of gelation through this process is less than obvious because each time one create a new branching by transesterification exchange, another link is broken somewhere.
In this circumstance, the relationship between composition and the possibility of gelation may be estimated using the Flory-Stockmayer model:[54, 55]

$$p = \frac{1}{\sqrt{r(1-f_A)(1-f_B)}} \qquad (1)$$

Where p is the extent of reaction at the gel point, f_A and f_B the average functionality of the monomers carrying functions A and B respectively and r the stoichiometric ratio of functions A and B ($r \leq 1$). This model was developed for polycondensation, it assumes equireactivity throughout the process and absence of loops but makes no hypothesis with regards to the chronology of forming bonds. For gelation to take place, equation 1 must have a solution with $p < 1$.
Once transesterification is activated, the diglycol units generated by opening the diepoxide monomers can exist in the form of mono-, di- tri- and tetra-esters as well as the free diglycol form (scheme 2).

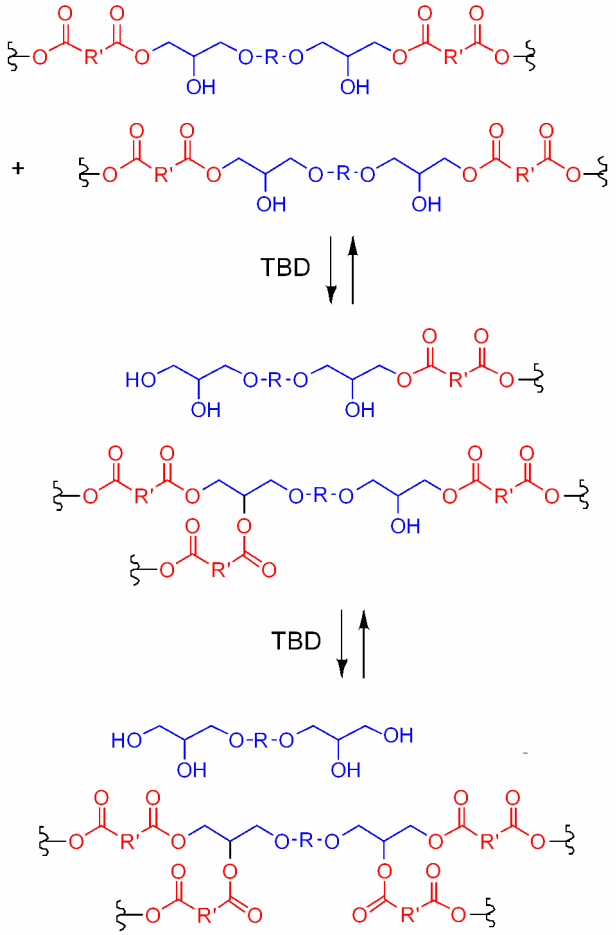

Scheme 2 Branching by transesterification mechanism, leading to exchangeable cross-links. The scheme illustrates the equilibrium between mono-, di-, tri-, tetraesters and the free diglycol form.

The diglycol unit therefore expresses a functionality $f_B = 4$, while it remained bifunctional in the absence of transesterification. If assuming equi-reactivity of all alcohol groups, transesterification of the (1:1) composition would reach the same equilibrium as condensation of one mol diacid with one mole diglycol where equation (1) with $f_A = 2$, $f_B = 4$ and $r = 0.5$ predicts gelation.[52] For the (1:0.75) composition, $r = 0.375$, gelation is still predicted but requires a high value of conversion ($p = 0.94$). For compositions farther from stoichiometry, 1:0.6, 1:0.5, 1:0.3 gelation would not take place if additions and transesterifications were the only reactions to occur.Gelation of polyhydroxyesters formed by 1:1 amounts of diepoxides and dicarboxylic acids has been investigated both theoretically and experimentally.[41, 42, 52, 56, 57] Further statistical study, based on the branching theory[57] also confirms the passage of the gel point in a diacid-diepoxide system able to reorganise.

Reaction 4 (chain polymerisation by anionic ROP), illustrated in Scheme 3, is likely to occur in a basic environment and promote gelation whenever epoxy is in excess. Additional links thereby formed are not ester but non-exchangeable ether links. Regarding this reaction, the diepoxide monomer is tetrafunctional and able to form crosslinks. Previous observations[41, 42] demonstrate that epoxy vitrimer formulations containing an 1:2 excess of epoxy and 1-methyl imidazole as initiator form networks though this reaction.

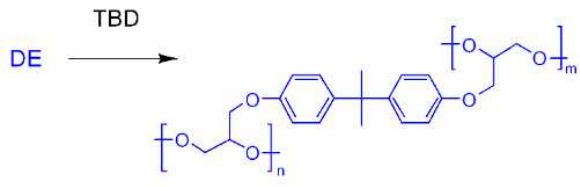

Scheme 3 Branching mechanism via anionic ROP of diepoxides -Ether bonds thereby formed are not exchangeable.

With TBD, reaction 3 (transesterification) is known to be fast[49, 52, 53] and allows the gel point to be passed quickly, while reaction 2 (Fischer esterification) and reaction 4 are slow but increase the crosslink density of the 3D network. Reactions 1 and 2 terminate when there is no more acid, whereas reaction 4 continues until there is no epoxy left and slows down with decrease of epoxy concentration. Therefore, in all samples with TBD and excess of epoxy the formation of the network is associated with reactions 1, 3 and 4.

Curing in the presence of a catalyst which is at the same time a strong base still questions whether the epoxy homopolymerisation can take place rather than the addition reaction between acid and epoxy. Hence, curing of epoxy was investigated by comparing the differences in evolution of IR signals for 30H5CAT-type compositions containing an (100:30) excess of epoxy mixed with 5% meq of either TBD or 2-PI. 2-PI is known to be an effective initiator for anionic ROP of epoxides.[37] Variations of IR signals for TBD and 2-PI based samples are plotted in Fig. 2c-d and in Fig. 3 respectively, using the same scales as Fig 2.

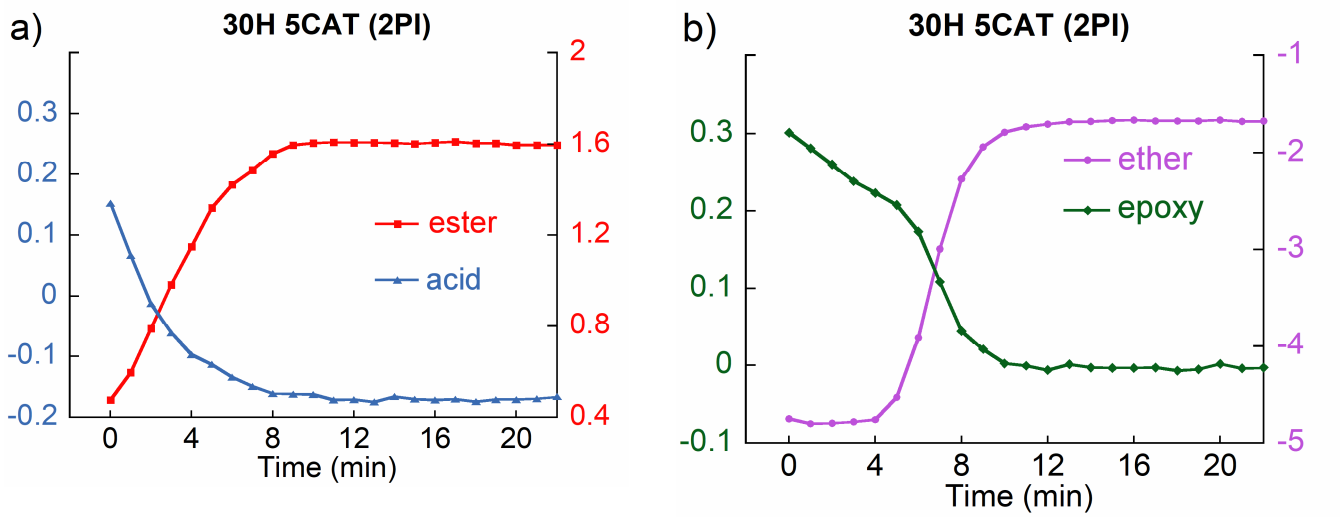

Fig. 3. Evolution of IR signals for a reactive composition containing a) an (100:30) molar excess of epoxy and b) 5 mol% of 2-PI as catalyst. Same Y-scales as Figure 2.

With 2-PI, the ester and acid traces mirror each other (Fig 3a) and reach complete conversion within about 8 minutes. As for the ether signal, it shows first an induction period of about 5 minutes, then a steep increase correlated with the disappearance of COOH functions and eventually saturation after about 12 min. As for the signal of the epoxy, it clearly shows two different slopes for both above reactions, first a slow conversion stage during reaction with the acid then a faster stage during anionic homopolymerisation.

If we compare with 2PI, the speed of reactions is overall slower with TBD, the two reactions are more clearly decoupled with 2PI but in both cases, the scenario is the same: a first wave is observed, corresponding to the addition reactions (Fig 2a and fig 2b) then a second wave due to anionic homopolymerisation. The proposed mechanism is very similar to that depicted in scheme 1 and scheme 2 in ref.[58] for a thiol-epoxy system. The base (either TBD or 2-PI) deprotonates the COOH function, producing a carboxylate anion which can attack the epoxy group and produce an alkoxide anion. In the presence of excess acid groups, a rapid proton exchange between the alkoxide anion and the acid takes place (because of the difference in pka of the

alcohol/alkoxide and acid/carboxylate pairs) leading to the formation of another carboxylate anion and a hydroxyester group. In off-stoichiometric formulations, once the acid is depleted this proton transfer does not take place and epoxy homopolymerisation propagates as long as alkoxide anions are present.
Once the acid is exhausted (after approx. 4 min for 2-PI, 12 min for TBD) conversion of epoxy accelerates with 2-PI (Fig 3b) while nothing similar happens with TBD (Fig 2d). 2-PI is known as nucleophile, able to directly attack the epoxy through formation of a zwitterionic adduct[59] and regenerating after ROP propagation,[60, 61] a mechanism consistent with acceleration after acid consumption. In TBD, the nucleophilic imine function neighbours with a H-bonding secondary amine function. This capping property is favourable to complex alkoxide and activated acyl functions at a suitable position for transesterification,[50] but may desactivate nucleophilic species involved in anionic ROP of epoxy.
On the other hand, TBD is significantly more basic than an imidazole (pKa of the conjugate acid > 20 for TBD[62] compared to a value of 6.48 for 2-PI[63]). TBD potentially attacks epoxy via the formation of oxygenated anions: alkoxide or carboxylate rather than directly.
The fact that homopolymerisation is slower with TBD increases probability of hydrolytic terminations e.g. with water molecules, conducive to appearance of additional hydroxyl groups able to participate in exchange reactions.

Swelling and soluble fraction analysis

The results of swelling experiments are summarised in Fig. 4. All samples swelled in TCB and remained insoluble indicating that network polymer chains are indeed in a good solvent environment and chemically bound to the rest of the network.

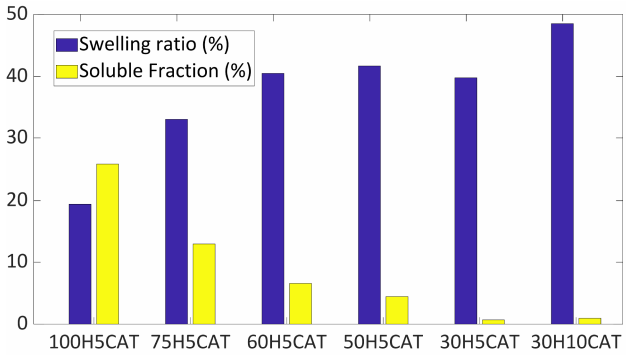

Fig. 4 Swelling experiment to confirm crosslinking of the structure, mass increase (blue) and mass fraction of the soluble part (yellow)

For 100H5CAT, the soluble fraction ≈25% is close to the predicted value.[57] The obtained network decreases its soluble fraction committedly with decrease in the acyl content of the samples, due to an increased crosslinking density and epoxy homopolymerisation. In contrary, the swelling ratio increases as the soluble fraction decreases with acyl content. It is notable that the 30H10CAT sample exhibited a slightly higher swelling ratio than 30H5CAT (≈ 49% against ≈ 40%). As shown below in DMA data, this difference correlates with a slightly lower elastic modulus of the former. This indicates a higher crosslink density when decreasing the amount of initiator for these off-stoichiometric compositions, where formation of the network is dominated by chainwise polymerisation. Overall, none of these samples were dissolved and are considered to have crosslinked beyond the gel point.

Mechanical properties at small and large deformations

DMA results, summarised in Fig. 5, show that when the acid content of the prepared vitrimers decreases (from 1:1 meq to 1:0.3 meq epoxy:acid), the glass transition temperature (tan delta peak values, Table S1) gradually increases, from ~ 40°C (sample 100H) to ~ 100°C (samples 30H). This variation follows the rule of mixtures described by the Fox-Flory equation, as also observed in off-stoichiometry thiol-epoxy formulation. [64, 65] thus demonstrating the homogeneity of the networks (Fig. S6). The catalyst loading (5% or 10% meq of epoxy) did not change the Tα of the 30H sample type but rubbery plateau modulus was lower with higher catalyst content. To summarise, it appears that Tα and the rubbery plateau can be tuned by changing the stoichiometric ratio between epoxy and hardener. It is worth noting that in our system the term “soft crosslinker” would be more appropriate than hardener.

The maximum of the loss tangent peak (Fig. 5b) gradually decreases concomitantly with sebacic acid content. This observation is to be correlated with the evolution of soluble fraction in the same series. Higher damping ability is related to the amount of network defects (i.e. dangling chains, isolated microgel fragments, oligomers). The presence of such defects in samples close to stoichiometry proves a crosslinking mechanism mostly related to exchanges by transesterification as illustrated in Scheme 3.

Whereas, off-stoichiometric compounds appear to be more tightly crosslinked, due to crosslinking mechanism by anionic ROP as illustrated in Scheme 2.

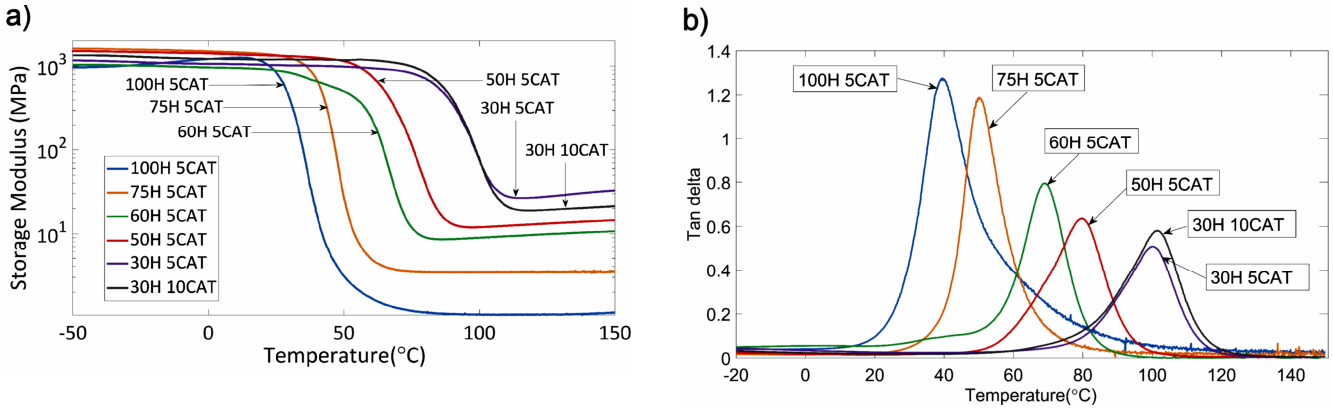

Fig. 5 a) Storage moduli for different ratios, obtained by DMA measurements; b) damping response of tested samples

Tensile tests were conducted and representative stress/strain curves for the different stoichiometric ratios investigated are presented in Fig. 6. Sample 100H5CAT exhibited significant elongation (>300%) and low stress at break (<2 MPa), and Young's modulus (0.5 MPa) corresponding to a lightly crosslinked elastomer. Once the content of acid is decreased (75H5CAT sample), the tensile response shows an increase of initial Young's modulus (1.6MPa) and strength (>10 MPa), and concomitant decrease in strain at break (~140%). At lower acid contents (50H5CAT and 30H5CAT), the materials behave like a stiff epoxy thermoset with a Young's modulus in the GPa range, and strength around 50 MPa.

The 100H5CAT behaves like a low-density crosslinked elastomer due to the length and size of the SA fragment and its relatively low T_α (~ 40°C). When the acid content is reduced, the homopolymerisation of epoxy leads to lower average distance between hard fragments of the epoxy backbone closely connected by glycerol units (Scheme 2). Contrary to SA/epoxy bonding that regularly introduced flexible spacer between them (Scheme 1 and Scheme 3).

Performance of off-stoichiometric samples are very similar to conventional epoxies used in industries, with sebacic acid being a relatively cheap and safe "hardener" to handle. Mechanical data are summarised in Table S2.

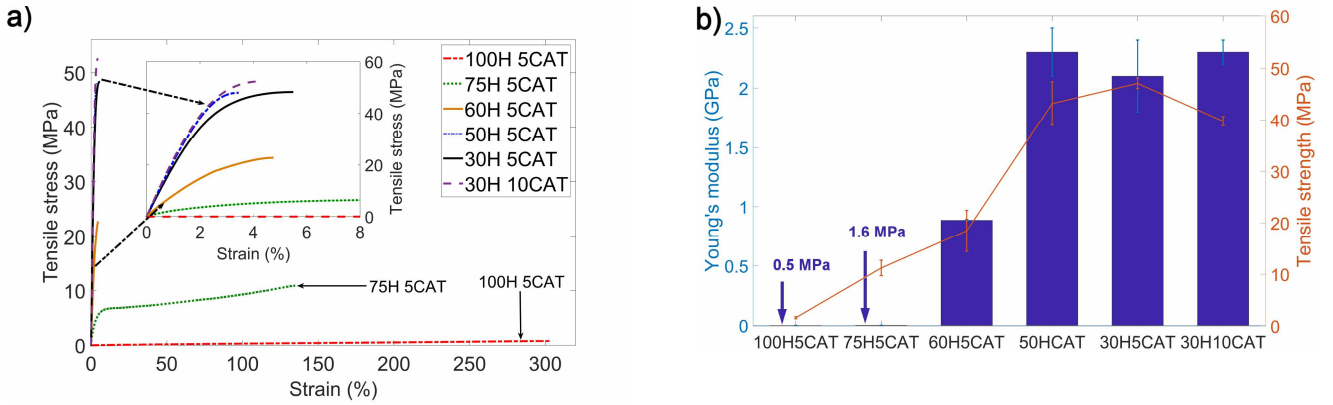

Fig. 6 Tensile behaviour obtained with ASTDM 638 type IV samples. a) Typical stress/strain curves obtained for each epoxy:acid ratio, b) Bar chart and curve comparing the Young's modulus and tensile strength of the samples

Stress relaxation of epoxy vitrimers

The capacity of relaxing stress was measured to ascertain the impact of off-stoichiometric formulation. The difference in mechanical properties required to adapt testing temperature for each sample examined (the stronger the network is, the higher temperature must be). Sample type 100H5CAT and 75H5CAT exhibit complete stress relaxation as shown in Fig. 7a and Fig. S7b. For 60H5CAT, at 180°C, the stress hardly relaxes down to 10% of the initial value after 20000s (Fig. 7.b) and application of higher temperature caused observable chemical degradation of the network and significant deviation from exponential decay at this time scale (Fig. S7c). Similar behaviour is observed for 50H5CAT sample with stress relaxed down to 20% of the initial value (Fig. S7d). 30H samples (5CAT and 10CAT) both exhibit a tendency to relax down to a value of $G/G_0 \approx 0.2$ (Fig. 7.c). These results are in line with the findings of Torkelson and coll.,[44] where vitrimers with < 50% of unexchangeable covalent were found to exhibit a near full relaxation. When the network is composed of more than 50% of irreversible bonds, it is only able to relax about 70% of the applied strain (30H 5CAT and 10CAT samples correspond to 70% irreversible covalent bond content in the network).

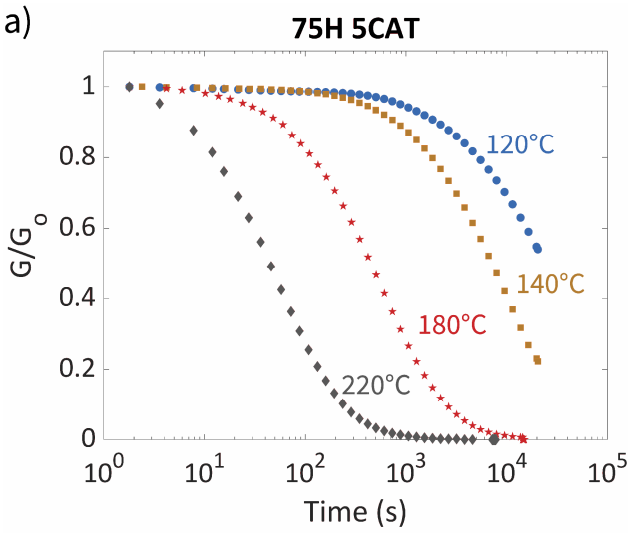

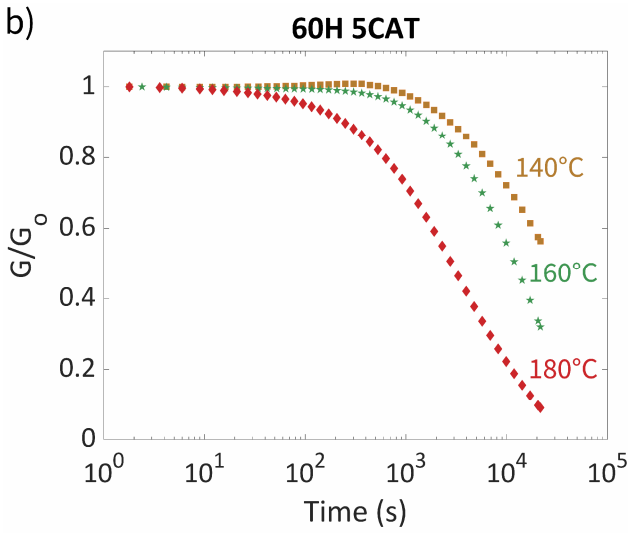

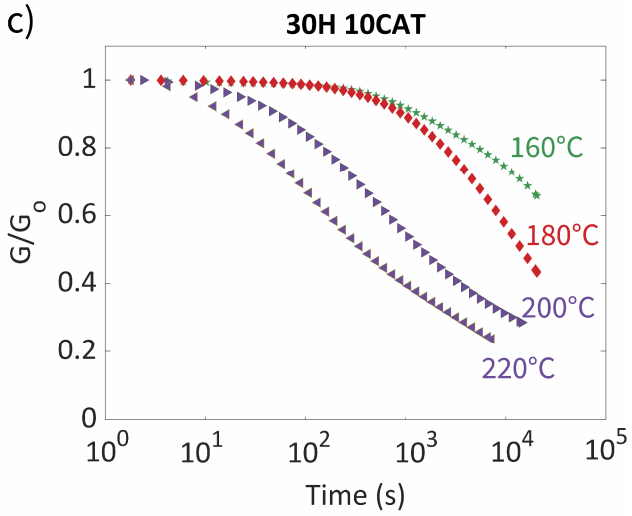

Fig. 7 Stress relaxation at different temperatures for three different epoxy/acid ratios: a) ratio 75H 5CAT, b) 60H5CAT, and c) ratio 30H10CAT

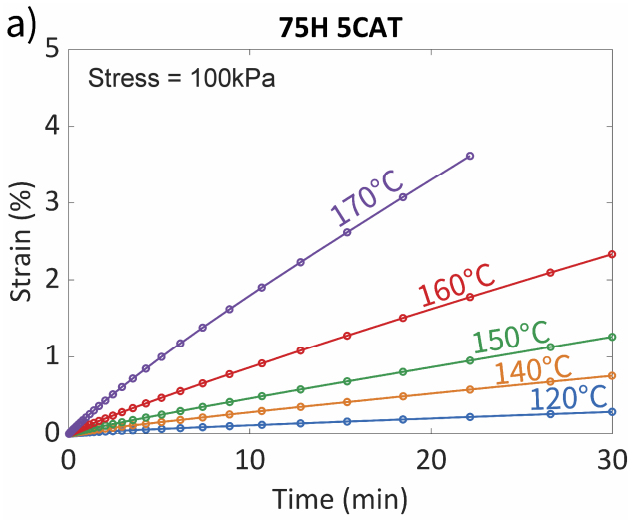

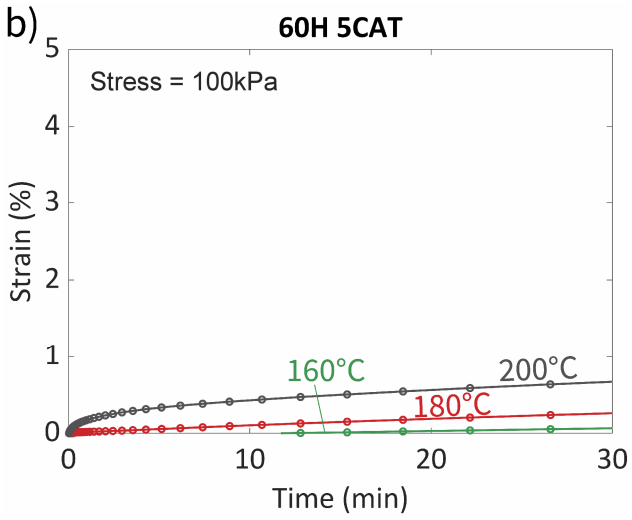

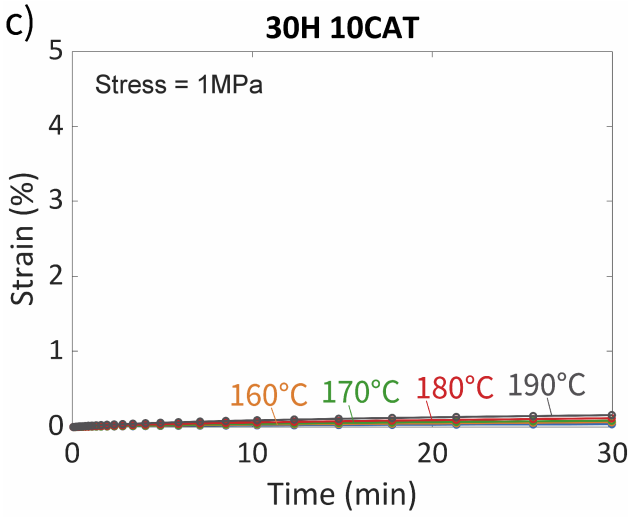

Fig. 8 Creep behaviour for different temperatures and three different epoxy/acid ratios: a) ratio 75H 5CAT, b) ratio 60H5CAT, and c) ratio 30H10CAT.

Creep behaviour of epoxy vitrimers

The flow properties of the materials were also evaluated using creep experiments. As pointed out recently, this method is useful to characterise vitrimers with very slow dynamics,[66] and avoids the shortcoming of low force measurements. Creep data of the same three samples under an applied stress of 0.1MPa (75H5CAT, 60H5CAT), and 1 MPa (30H10CAT) are presented in Fig. 8. Evidently, the sample closest to stoichiometry (75H5CAT, Fig.8a) flows like a liquid with a deformation increasing linearly with time, as also observed for 100H5CAT sample (Fig. S8b). Moving further towards off-stoichiometry samples (60H5CAT), creep data do not reveal a capacity to flow as the acquired deformation after 30min is still well below 1% and the overall variation is not linear with time. This demonstrates that despite its capacity to nearly relax full stress under 1% applied deformation, 60H5CAT is, however, unable to flow like a liquid. Such observations lead to the conclusion that this material cannot be recognised as vitrimer, but rather as vitrimer-like material as defined in refs [67, 68] showing the ability to be welded or healed but not entirely reshaped. Moving further to 50% and below of acyl content (50H5CAT, 30H5CAT and 30H10CAT), any ability to flow disappears from creep profiles (Fig. S8d, e and Fig. 8c) and the data rather suggest shape fixity of an essentially permanent network.
Fitting stress relaxation data of 100H5CAT by a single exponential decay allows to determine the relaxation time, e.g. at 180°C: τ ~ 90s. The value of τ at any temperature deduced from stress relaxation data is represented as Arrhenius plot in Fig. 9a. The slope gives an activation energy of about 100 kJ/mol.
Same treatment on 75H5CAT stress relaxation data afford significantly longer relaxation times e.g. τ ~ 700s at 180°C and a similar activation energy. In addition, experimental data do not completely overlap the fit, suggesting that more than one relaxation time had to be considered.
In figure 9b the Arrhenius plots of the same samples are calculated from creep data.
In this figure, the activation energy for 75h5CAT is lower and viscosity higher than the stoichiometric one. This indicate that the presence of sequences comprising a large number of non-exchangeable bonds induce slower relaxation modes which is not detectable by a monoexponential fit and decrease the themoresponsivity of the system.

In other samples 50H5CAT, 30H5CAT (Fig. S7d,e), 60H5CAT, and 30H10CAT (Fig. 7b and Fig. 7c), the extend of stress relaxation progressively decreases concomitantly with acid content and fitting by a single exponential model can no longer be achieved.

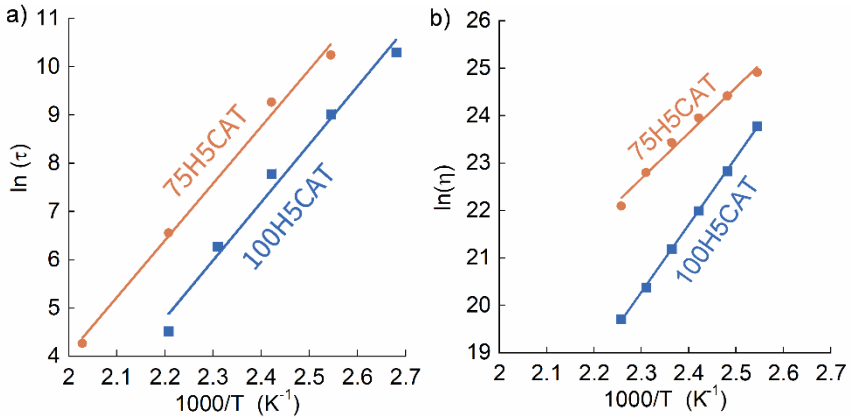

Fig. 9 Arrhenius plot from a) stress relaxation and b) creep data of vitrimers with two different epoxy/acid ratios.

Conclusions

The present work demonstrates that full conversation of epoxy functions is achieved despite using an acyl content relatively low compared to the epoxy amount (down to 30% of the epoxy functions). The side reactions involved in the cure of non-stoichiometric systems are not necessarily detrimental to materials properties. Effectively, the TBD promotes anionic ROP in off-stoichiometric samples, leading to branching and crosslinking of the network. However, this reaction remains slow compared to the polyaddition of epoxy and acyl functions and promotes the formation of non-exchangeable polyether chains. At any stoichiometry, the epoxy acyl curing in the presence of TBD produces an insoluble crosslinked polymer (> 75% of insoluble fraction). Samples closer to the stoichiometry present more defects compared to samples with strong off-stoichiometry composition, which explains the improvement of thermomechanical properties in the elastomeric range. The rubbery plateau and mechanical strength of the materials both increase when departing from stoichiometry and a transition from elastomeric to glassy behaviour is observed. This transition of the thermomechanical properties with the hardener content lead to conclude that the sebacic acid acts more as a “soft crosslinker” for this network. When decreasing the acyl content of the formulation, the network undergoes a progressive transition from a vitrimer material (100H5CAT and 75H5CAT), to a vitrimer-like[67, 68] material (60H5CAT), and finally, to permanent crosslinked material. The present study shows the potential to produce tunable vitrimer

formulation, without changing any of the manufacturing process parameters other than stoichiometry. This tuning aspect could raise practical interests for applications requiring tailored thermomechanical properties, without the need of altering the chemical formulation or handling processes.

Conflicts of interest

There are no conflicts to declare.

Author information

*corresponding authors: francois.tournilhac@espci.fr, matthieu.gresil@monash.edu

ORCID
Francois Tournilhac: 0000-0002-6775-1584
Matthieu Gresil: 0000-0002-3593-2655
Constantinos Soutis: 0000-0002-1402-9838
Jonny Blaker: 0000-0003-1112-8619
Quentin-Arthur Poutrel: 0000-0002-4059-2173

Acknowledgements

We thank Polly Greensmith and Mickael Pomes-Hadda for their technical assistance with DMA. F.T. acknowledge financial support from ANR through the MATVIT project (ANR-18-CE06-0026-01) and the European Union's Horizon 2020 research and innovation program under grant agreement No. 828818.

References

1. L. Leibler, M. Rubinstein and R. H. Colby, *Journal Physics II*, 1993, **3**, 1581-1590.
2. R. D. Andrew, A. V. Tobolsky and E. E. Hanson, *Rubber Chemistry and Technology*, 1946, **4**, 1099-1112.
3. C. N. Bowman and C. J. Kloxin, *Angewandte Chemie - International Edition*, 2012, **51**, 4272-4274.
4. C. J. Kloxin and C. N. Bowman, *Chem Soc Rev*, 2013, **42**, 7161-7173.
5. X. Chen, M. A. Dam, K. Ono, A. Mal, H. Shen, S. R. Nutt, K. Sheran and F. Wudl, *Science*, 2002, **295**, 1698.
6. V. Froidevaux, M. Borne, E. Laborbe, R. Auvergne, A. Gandini and B. Boutevin, *RSC Advances*, 2015, **5**, 37742-37754.
7. A. Gandini, *Progress in Polymer Science*, 2013, **38**, 1-29.
8. T. F. Scott, A. D. Schneider, W. D. Cook and C. N. Bowman, *Science*, 2005, **308**, 1615.
9. D. Montarnal, M. Capelot, F. Tounilhac and L. Leibler, *Science*, 2011, **334**, 965-968.
10. M. Capelot, D. Montarnal, F. Tournilhac and L. Leibler, *Journal of the American Chemical Society*, 2012, **134**, 7664-7667.
11. R. L. Snyder, D. J. Fortman, G. X. De Hoe, M. A. Hillmyer and W. R. Dichtel, *Macromolecules*, 2018, **51**, 389-397.
12. Y. Spiesschaert, M. Guerre, L. Imbernon, J. M. Winne and F. Du Prez, *Polymer*, 2019, **172**, 239-246.
13. I. Azcune and I. Odriozola, *European Polymer Journal*, 2016, **84**, 147-160.
14. L. Zhang and S. J. Rowan, *Macromolecules*, 2017, **50**, 5051-5060.
15. S. Zhang, L. Pan, L. Xia, Y. Sun and X. Liu, *Reactive and Functional Polymers*, 2017, **121**, 8-14.
16. B. Hendriks, J. Waelkens, J. M. Winne and F. E. Du Prez, *ACS Macro Letters*, 2017, **6**, 930-934.
17. M. M. Obadia, A. Jourdain, P. Cassagnau, D. Montarnal and E. Drockenmuller, *Advanced Functional Materials*, 2017, **27**, 1703258.
18. A. Demongeot, R. Groote, H. Goossens, T. Hoeks, F. Tournilhac and L. Leibler, *Macromolecules*, 2017, **50**, 6117-6127.
19. J. Tang, L. Wan, Y. Zhou, H. Pan and F. Huang, *Journal of Materials Chemistry A*, 2017, **5**, 21169-21177.
20. T. Stukenbroeker, W. Wang, J. M. Winne, F. E. Du Prez, R. Nicolaÿ and L. Leibler, *Polymer Chemistry*, 2017, **8**, 6590-6593.
21. A. Arnebold, S. Wellmann and A. Hartwig, *Polymer*, 2016, **91**, 14-23.
22. A. Arnebold, S. Wellmann and A. Hartwig, *Journal of Applied Polymer Science*, 2016, **133**.
23. V. R. Sastri and G. C. Tesoro, *Journal of Applied Polymer Science*, 1990, **39**, 1439-1457.
24. J.-P. Pascault and R. J. J. Williams, *Epoxy Polymers: New Materials and innovations*, Wiley, 2010.
25. M. Holst, K. Schänzlin, M. Wenzel, J. Xu, D. Lellinger and I. Alig, *Journal of Polymer Science Part B: Polymer Physics*, 2005, **43**, 2314-2325.
26. X. Fernàndez-Francos, S. G. Kazarian, X. Ramis and À. Serra, *Applied Spectroscopy*, 2013, **67**, 1427-1436.
27. J. Scheirs and T. E. Long, *Modern Polyesters: Chemistry and Technology of Polyesters and Copolyesters; Chap II and V*, John Wiley and Sons Ltd., Chichester, 2003.
28. M. Delahaye, J. M. Winne and F. E. Du Prez, *Journal of the American Chemical Society*, 2019, **141**, 15277-15287.
29. F. Ma and M. A. Hanna, *Bioresource Technology*, 1999, **70**, 1-15.
30. W. Liu, D. F. Schmidt and E. Reynaud, *Industrial & Engineering Chemistry Research*, 2017, **56**, 2667-2672.
31. M. Capelot, M. M. Unterlass, F. Tournilhac and L. Leibler, *ACS Macro Letters*, 2012, **1**, 789-792.

32. A. S. Hoffman, *Advanced Drug Delivery Reviews*, 2013, **65**, 10-16.
33. J. Otera, *Chemical Reviews*, 1993, **93**, 1449-1470.
34. A. Demongeot, S. J. Mougnier, S. Okada, C. Soulié-Ziakovic and F. Tournilhac, *Polymer Chemistry*, 2016, **7**, 4486-4493.
35. E. Chabert, J. Vial, J.-P. Cauchois, M. Mihaluta and F. Tournilhac, *Soft Matter*, 2016, **12**, 4838-4845.
36. A. Ruiz de Luzuriaga, R. Martin, N. Markaide, A. Rekondo, G. Cabañero, J. Rodríguez and I. Odriozola, *Materials Horizons*, 2016, **3**, 241-247.
37. V. Rebizant, A.-S. Venet, F. Tournilhac, E. Girard-Reydet, C. Navarro, J.-P. Pascault and L. Leibler, *Macromolecules*, 2004, **37**, 8017-8027.
38. Q. Shi, K. Yu, X. Kuang, X. Mu, C. K. Dunn, M. L. Dunn, T. Wang and H. Jerry Qi, *Materials Horizons*, 2017, **4**, 598-607.
39. Y. Yang, Z. Pei, X. Zhang, L. Tao, Y. Wei and Y. Ji, *Chemical Science*, 2014, **5**, 3486-3492.
40. K. Yu, P. Taynton, W. Zhang, M. L. Dunn and H. J. Qi, *RSC Advances*, 2014, **4**, 48682-48690.
41. F. I. Altuna, C. E. Hoppe and R. J. J. Williams, *RSC Advances*, 2016, **6**, 88647-88655.
42. F. Altuna, C. Hoppe and R. Williams, *Polymers*, 2018, **10**, 43.
43. L. Matějka, S. Pokomý and K. Dušek, *Polymer Bulletin*, 1982, **7**, 123-128.
44. L. Li, X. Chen, K. Jin and J. M. Torkelson, *Macromolecules*, 2018, **51**, 5537-5546.
45. C. E. Hoppe, M. J. Galante, P. A. Oyanguren and R. J. J. Williams, *Macromolecular Materials and Engineering*, 2005, **290**, 456-462.
46. F. I. Altuna, C. E. Hoppe and R. J. J. Williams, *European Polymer Journal*, 2019, **113**, 297-304.
47. Z. Pei, Y. Yang, Q. Chen, E. M. Terentjev, Y. Wei and Y. Ji, *Nature Materials*, 2014, **13**, 36-41.
48. Z. Pei, Y. Yang, Q. Chen, Y. Wei and Y. Ji, *Advanced Materials*, 2016, **28**, 156-160.
49. B. G. G. Lohmeijer, R. C. Pratt, F. Leibfarth, J. W. Logan, D. A. Long, A. P. Dove, F. Nederberg, J. Choi, C. Wade, R. M. Waymouth and J. L. Hedrick, *Macromolecules*, 2006, **39**, 8574-8583.
50. R. C. Pratt, B. G. G. Lohmeijer, D. A. Long, R. M. Waymouth and J. L. Hedrick, *Journal of the American Chemical Society*, 2006, **128**, 4556-4557.
51. E. Cazares-Cortes, B. C. Baker, K. Nishimori, M. Ouchi and F. Tournilhac, *Macromolecules*, 2019, **52**, 5995-6004.
52. M. Capelot, *Chimie de Polycondensation, Polymères Supramoléculaires et Vitrimères* Thèse, Université Pierre et Marie Curie - Paris VI, 2013.
53. U. Schuchardt, R. Sercheli and R. M. Vargas, *Journal of the Brazilian Chemical Society*, 1998, **9**, 199-210.
54. P. J. Flory, *Journal of the American Chemical Society*, 1941, **63**, 3083-3090.
55. W. H. Stockmayer, *The Journal of Chemical Physics*, 1944, **12**, 125-131.
56. J. E. Klee, F. Claußen and H. H. Hörhold, *Polymer Bulletin*, 1995, **35**, 79-85.
57. K. Dusek and L. Matejka, in *Rubber-Modified Thermoset Resins*, American Chemical Society, 1984, vol. 208, ch. 2, pp. 15-26.
58. X. Fernández-Francos, A.-O. Konuray, A. Belmonte, S. De la Flor, À. Serra and X. Ramis, *Polymer Chemistry*, 2016, **7**, 2280-2290.
59. M. S. Heise and G. C. Martin, *Macromolecules*, 1989, **22**, 99-104.
60. X. Fernàndez-Francos, *European Polymer Journal*, 2014, **55**, 35-47.
61. S. K. Ooi, W. D. Cook, G. P. Simon and C. H. Such, *Polymer*, 2000, **41**, 3639-3649.
62. I. Kaljurand, A. Kütt, L. Sooväli, T. Rodima, V. Mäemets, I. Leito and I. A. Koppel, *The Journal of Organic Chemistry*, 2005, **70**, 1019-1028.
63. H. Walba and R. W. Isensee, *The Journal of Organic Chemistry*, 1961, **26**, 2789-2791.
64. T. G. Fox and P. J. Flory, *Journal of Applied Physics*, 1950, **21**, 581-591.
65. A. Belmonte, C. Russo, V. Ambrogi, X. Fernández-Francos and S. De la Flor, *Polymers*, 2017, **9**, 113.
66. R. G. Ricarte, F. Tournilhac, M. Cloître and L. Leibler, *Macromolecules*, 2020, **53**, 1852-1866.
67. L. Imbernon, S. Norvez and L. Leibler, *Macromolecules*, 2016, **49**, 2172-2178.
68. S. Kaiser, S. Wurzer, G. Pilz, W. Kern and S. Schlögl, *Soft Matter*, 2019, **15**, 6062-6072.